Evidence for a Catalytic Mg^{2+} Ion and Effect of Phosphate on the Activity of *Escherichia coli* Phosphofructokinase-2: Regulatory Properties of a Ribokinase Family Member†

Rafael E. Parducci, Ricardo Cabrera, Mauricio Baez, and Victoria Guixé*

Departamento de Biología, Facultad de Ciencias, Universidad de Chile, Casilla 653, Santiago, Chile

Received January 5, 2006; Revised Manuscript Received April 20, 2006

ABSTRACT: Phosphofructokinase-2 (Pfk-2) from *Escherichia coli* belongs to the ribokinase family of sugar kinases. One of the signatures observed in amino acid sequences from the ribokinase familiy members is the NXXE motif, which locates at the active site in the ribokinase fold. It has been suggested that the effect of Mg^{2+} and phosphate ions on enzymatic activity, observed in several adenosine kinases and ribokinases, would be a widespread feature in the ribokinase family, with the conserved amino acid residues in the NXXE motif playing a role in the binding of these ions at the active site [Maj, M. C., et al. (2002) *Biochemistry 41,* 4059−4069]. In this work we study the effect of Mg^{2+} and phosphate ions on Pfk-2 activity and the involvement of residue E190 from the NXXE motif in this behavior. The kinetic data are in agreement with the requirement of a Mg^{2+} ion, besides the one present in the metal−nucleotide complex, for catalysis in the wild-type enzyme. Since the response to free Mg^{2+} concentration is greatly affected in the E190Q mutant, we conclude that this residue is required for the proper binding of the catalytic Mg^{2+} ion at the active site. The E190Q mutant presents a 50-fold decrease in the k_{cat} value and a 15-fold increment in the apparent K_m for $MgATP^{2-}$. Inorganic phosphate, typically considered an activator of adenosine kinases, ribokinases, and phosphofructokinases (nonhomologous to Pfk-2) acted as an inhibitor of wild-type and E190Q mutant Pfk-2. We suggest that phosphate can bind to the allosteric site of Pfk-2, producing an inhibition pattern qualitatively similar to $MgATP^{2-}$, which can be reversed to some extent by increasing the concentration of fructose-6-P. Given that the E190Q mutant presents alterations in the inhibition by $MgATP^{2-}$ and phosphate, we conclude that the E190 residue has a role not only in catalysis but also in allosteric regulation.

The members of the ribokinase family of sugar kinases catalyze the phosphorylation of substrates containing a secondary hydroxyl group. This family includes kinases of adenosine, fructose, tagatose-6-P, fructose-6-P, and fructose-1-P, in addition to ribokinase, the canonical enzyme (*1*, *2*). The structure of some of the members is known in atomic detail, providing useful insights about the function of conserved amino acid residues in catalysis and substrate-induced conformational changes (*3*−*8*). Folding conservation revealed by structure determination allowed recognizing distant homologues, including kinases involved in coenzyme metabolism (*9*−*11*), ADP-dependent glucokinases (*12*, *13*), and ADP-dependent phosphofructokinases (*14*). All of these kinases constitute a superfamily.

Activation and inhibition of enzymatic activity are common features among some of the members of the ribokinase family. For example, in the case of phosphofructokinase-2 (Pfk-2)[1] from *Escherichia coli*, a member of the ribokinase family, the binding of the substrate $MgATP^{2-}$ to an allosteric site causes inhibition of the enzymatic activity and association of the native dimers into tetramers (*15*−*17*). On the basis of homology modeling and X-ray scattering experiments, we have characterized the structural changes associated with the allosteric binding of $MgATP^{2-}$ (*18*). Bacterial ribokinase is affected by pentavalent ions such as phosphate, arsenate, and vanadate, which increase both the velocity and the affinity of the enzyme for ribose (*19*). Also, structural evidence for conformational changes associated to the activation by potassium in bacterial ribokinase has been obtained by X-ray crystallographic studies (*20*). Regarding adenosine kinase, a strong inhibition is observed at high concentrations of its substrate adenosine. Conversely, stimulation of enzyme activity by phosphate and other pentavalent ions has been demonstrated for adenosine kinase from several sources (*21*). At low concentrations, free Mg^{2+} activates adenosine kinase; however, at the milimolar range it behaves as an inhibitor and increases the substrate inhibition induced by adenosine (*22*). It seems that phosphate antagonizes the effect of Mg^{2+} on adenosine kinase activity, given the reduced level of inhibition observed in the presence of this ion (*21*).

The NXXE motif, conserved among the members of the superfamily, has been suggested to play a role in the mechanism by which Mg^{2+} and phosphate ions affect the

† This work was supported by a grant from the Fondo Nacional de Desarrollo Científico y Tecnológico (Fondecyt 1040892).

* To whom correspondence should be addressed. Fax: 56-2-2712983. Phone: 56-2-9787335. E-mail: vguixe@uchile.cl.

[1] Abbreviations: DTT, dithiothreitol; HPLC, high-performance liquid chromatography; R_S, Stokes radius; ATP_t, total concentration of ATP; Mg_t, total concentration of Mg^{2+}; PVI, pentavalent ions; Pfk-2, phosphofructokinase-2.

10.1021/bi060026o CCC: $33.50
Published on Web 07/11/2006

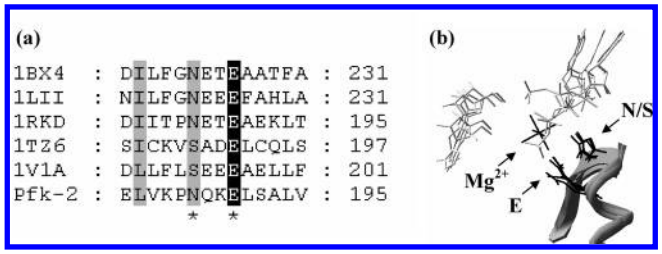

FIGURE 1: (a) Sequence alignment obtained from the structural superposition of crystallographic structures of adenosine kinases from *H. sapiens* (1bx4) and *T. gondii* (1lii), ribokinase from *E. coli* (1rkd), AIR kinase from *S. enterica* (1tz6), and 2-keto-3-deoxygluconate kinase from *T. thermophilus* (1v1a) and the sequence of Pfk-2 from *E. coli*. Conserved and identical residues are highlighted in gray and black, respectively. N/S and E from the NXXE motif are marked with an asterisk. (b) Structural superposition of 1bx4, 1lii, 1rkd, 1tz6, and 1v1a around the NXXE motif. Side chains of the residues marked with an asterisk in (a) are shown in black. Mg^{2+} ion from 1bx4 is also shown in black. Active site ligands are shown in light gray.

activity of adenosine kinase (*21*) (Figure 1a). The residues of this motif are located at the active site in all of the known structures of members of the superfamily (Figure 1b). The mutation of N in the NXXE motif of wild-type adenosine kinase produces a marked reduction in the affinity for the substrates, adenosine and ATP, and the loss of the phosphate-induced activation (*21*). Also, the replacement of E from the NXXE motif by D or L produces enzymes which are more active in the absence of phosphate but are less activated in the presence of this ligand. In the absence of phosphate, the affinity for the activating Mg^{2+} was affected by either N or E mutations, and this effect was correlated to attenuation in the Mg^{2+}-induced inhibition, with N mutants displaying the major effect. In the presence of phosphate the results are less straightforward since the inhibition by free Mg^{2+} was enhanced, abolished, or unaffected by phosphate without a clear pattern. The observations of Maj et al. (*21*) support the view that N and E from the NXXE motif play an important role in phosphate and Mg^{2+} binding to the active site of adenosine kinase.

While essentially all kinases require a Mg^{2+}−nucleotide complex as one of the substrates, an additional divalent cation is required in some kinases for full activity, as observed with pyruvate kinase (*23*), phosphoenolpyruvate kinase (*24*), and extracellular regulated protein kinase-2 (*25*). While it was demonstrated that the true substrate for Pfk-2 is $MgATP^{2-}$ and not ATP^{4-} (*15*), it is not known if only this Mg^{2+} is required for catalysis and which are the residues involved in Mg^{2+} binding at the active site. Mg^{2+} has been demonstrated to be important for efficient catalysis in the nonhomologous phosphofructokinase-1 (Pfk-1), the other isozyme present in *E. coli*. Mutation of the conserved D129 to S in this enzyme causes a large reduction in catalytic rate, suggesting that the carboxylate group from D is important for the correct positioning of the Mg^{2+} ion (*26*).

In this work we tested the hypothesis that free Mg^{2+} and phosphate are general effectors of the ribokinase family members using Pfk-2 as an example of a member whose activity is an essential step in the glycolytic pathway. Also, we evaluated the role of residue E190 from the NXXE motif of Pfk-2 on the sensitivity of this enzyme to Mg^{2+} and phosphate. Our results indicate that a catalytic Mg^{2+} ion, additional to that present in the $MgATP^{2-}$ complex, is important for enzymatic activity and that E190 participates in the interaction with this ion. Also, we show that phosphate behaves as an inhibitor of wild-type and E190Q mutant Pfk-2, resembling the inhibition induced by MgATP. This result is opposite to the effect observed for phosphate in other phosphofructokinases and ribokinase family members.

EXPERIMENTAL PROCEDURES

Site-Directed Mutagenesis of Pfk-2. Site-directed mutagenesis of Glu 190 was carried out using the QuickChange (Stratagene) system using a pET21d plasmid (Novagen) containing the *pfk-2* gene as template. Two oligonucleotides were used to construct the E190Q mutant, both complementary to opposite strands of the template. The bold letter indicates the substituted base, and underlined bases indicate the codon for the newly introduced amino acid (only "sense" oligonucleotides are shown): 5′-G GTT AAG CCT AAC CAA AAA **C**AA CTC AGT GCG CTG GTG AAT CG-3′. The changed bases were verified by DNA sequencing of the mutant.

Enzyme Expression and Purification. The mutant Pfk-2 enzyme was produced in *E. coli* DF1020 since this strain does not express wild-type phosphofructokinases (*27*). DF1020 strain was cotransformed with plasmid pGP1-2 (*28*) that allows the expression of the T7 RNA polymerase after heat induction and the pET21d plasmid carrying the Pfk-2 wild-type or mutated gene. Cultures were grown at 30 °C in Luria broth media supplemented with ampicillin and kanamycin to a final concentration of 100 and 75 μg/mL, respectively. Protein expression was induced when the $A_{600} = 0.5$ by heat treatment at 42 °C for 20 min; thereafter, the culture was incubated at 37 °C for 4 h before the cells were collected by centrifugation. Wild-type and E190Q mutant Pfk-2 were purified essentially as described in Babul (*29*), replacing the AMP−agarose step with a second chromatography in Cibacron blue−Sepharose. The transformed *E. coli* strains produced an average of 10−15 mg of protein (wild-type and mutant Pfk-2) per liter of culture.

Enzyme Assay. Phosphosfructokinase activity was determined spectrophotometrically by coupling the fructose-1,6-bisphosphate production to the oxidation of NADH at pH 8.2, as described previously (*29*). The concentration of Mg^{2+}, ATP^{4-}, and $MgATP^{2-}$ was calculated from the total concentration of the nucleotide (ATP_t) and divalent cation (Mg_t) used in the assay, assuming a dissociation constant of 14 μM for the ionic equilibrium $MgATP^{2} \leftrightarrow ATP^{4-} + Mg^{2+}$ (*30*). The ionic species present in solution were calculated by using the quadratic solution:

$$[MgATP^{2-}] = \{([ATP]_t + [Mg]_t + 14) - \sqrt{([ATP]_t + [Mg]_t + 14)^2 - 4[ATP]_t[Mg]_t}\}/2 \quad (1)$$

$$[Mg^{2+}] = [Mg]_t - [MgATP^{2-}] \quad (2)$$

$$[ATP^{4-}] = [ATP]_t - [MgATP^{2-}] \quad (3)$$

Protonated forms of the nucleotide, such as $HATP^{3-}$ or H_2ATP^{2-}, are poorly represented at pH 8.2, so their concentration is not considered here.

Analysis of Kinetic Data. The initial rate was obtained as a function of ATP_t concentration at several but fixed Mg_t

Model I

$$\text{E-F6P} + Mg^{2+} \overset{K_{Mg}}{\leftrightarrow} \text{E-F6P-}Mg^{2+} + MgATP^{2-} \overset{K_m}{\leftrightarrow} \text{E-F6P-}Mg^{2+}\text{-MgATP}^{2-} \rightarrow \text{Product}$$

$$+$$

$$ATP^{4-} \overset{Ki}{\leftrightarrow} \text{E-F6P-}Mg^{2+}\text{-}ATP^{4-}$$

Model II

$$\text{E-F6P} + Mg^{2+} \overset{K_{Mg}}{\leftrightarrow} \text{E-F6P-}Mg^{2+} + MgATP^{2-} \overset{K_m}{\leftrightarrow} \text{E-F6P-}Mg^{2+}\text{-MgATP}^{2-} \rightarrow \text{Product}$$

$$+ \qquad\qquad\qquad\qquad\qquad\qquad \updownarrow K_{Mg2}$$

$$MgATP^{2-} \leftrightarrow \text{E-F6P-MgATP}^{2-} + Mg^{2+}$$

concentrations. This scheme generates mixtures of Mg^{2+}, $MgATP^{2-}$, and ATP^{4-} that were used to evaluate several models. Equations 1−3 were used to incorporate the equilibrium concentrations of $MgATP^{2-}$, Mg^{2+}, and ATP^{4-} into each model. Two models of activation by Mg^{2+} were found to account for the experimental data. In both models the free enzyme indeed represents the complex E−fructose-6-P, since the enzymatic activity was obtained in the presence of 1 mM fructose-6-P for all tested conditions. The first model (see Model I) involves an essential activation by Mg^{2+}, since it is required for ATP^{4-} and $MgATP^{2-}$ binding to the Pfk-2−fructose-P complex (*31*).

In this case, ATP^{4-} acts as a competitive inhibitor because the E−fructose-6-P−Mg^{2+}−ATP^{4-} complex is inactive. Conversely, the E−fructose-P−Mg^{2+}−$MgATP^{2-}$ complex is considered as the catalytic species. The equation derived from rapid equilibrium assumptions is showed in terms of free ligand concentrations:

$$v = \frac{k_{cat}E\dfrac{[Mg^{2+}][MgATP^{2-}]}{K_{Mg}K_m}}{1 + \dfrac{[Mg^{2+}]}{K_{Mg}}\left(1 + \dfrac{[ATP^{4-}]}{K_i} + \dfrac{[MgATP^{2-}]}{K_m}\right)}$$

In the second model (see Model II), Mg^{2+} binding is not required for $MgATP^{2-}$ binding to the E−fructose-6-P complex, but it is necessary to form the catalytically competent E−fructose-6-P−Mg^{2+}−$MgATP^{2-}$ complex (*32*). In this case, the inhibition by ATP^{4-} was not considered.

Under rapid equilibrium conditions the rate equation in terms of free ligand concentrations is

$$v = k_{cat}E[Mg^{2+}][MgATP^{2-}]/\{K_m[Mg^{2+}] + K_mK_{Mg} + [MgATP^{2-}][Mg^{2+}] + K_{Mg2}[MgATP^{2-}]\}$$

The equilibrium constants derived from the rapid equilibrium assumption for both models are

$$K_m = \frac{[E\cdot Mg^{2+}][MgATP^{2-}]}{[E\cdot Mg\cdot MgATP^{2-}]}$$

$$K_{Mg} = \frac{[E][Mg^{2+}]}{[E\cdot Mg^{2+}]}$$

$$K_i = \frac{[E\cdot Mg^{2+}][ATP^{4-}]}{[E\cdot Mg^{2+}\cdot ATP^{4-}]}$$

$$K_{Mg2} = \frac{[E\cdot MgATP^{2-}][Mg^{2+}]}{[E\cdot Mg^{2+}\cdot MgATP^{2-}]}$$

The experimental curves were simultaneously fitted to each model (and others not shown) by using Sigma-plot software 9.0 (Systat Software, Inc.).

Size Exclusion Chromatography. Experiments were performed with a Waters 1525 HPLC binary pump system, with a Bio-Sil SEC-250 (7.8 mm × 30 cm) column (Bio-Rad, Hercules, CA) equilibrated in a buffer containing 25 mM Tris-HCl, pH 7.5, 200 mM KCl, and 2 mM DTT in the presence of 1 or 30 mM $MgCl_2$ at the indicated $MgATP^{2-}$ concentrations. All runs were carried out at a flow rate of 0.8 mL/min. The column was calibrated with the following molecular mass markers: vitamin B_{12} (1.35 kDa, 8.5 Å R_S), horse myoglobin (17 kDa, 19 Å R_S), chicken ovalbumin (44 kDa, 30.5 Å R_S), bovine γ-globulin (158 kDa, 41.8 Å R_S), and bovine thyroglobulin (670 kDa, 85 Å R_S). Protein elution was recorded with the use of an online Waters 2487 UV dual detector measuring the absorbance at 280 nm. Since an increment in the ionic strength with the Mg^{2+} concentration causes displacements of the elution volume of the standards, a calibration curve for each Mg^{2+} concentration was constructed.

RESULTS

Effect of Free Mg^{2+} on the Catalytic Properties of Pfk-2 and the E190Q Mutant. To evaluate the effect of free Mg^{2+} on Pfk-2 activity, we follow an experimental setup in which the total concentration of Mg_t in the assay was held constant while the total concentration of ATP_t was increased from 0 to an excess over the total Mg_t concentration. In this way, the concentration of $MgATP^{2-}$ increases in the presence of free Mg^{2+} and, after titration of the total Mg^{2+}, the concentration ATP^{4-} increases over the metal−nucleotide substrate complex. Accordingly, the initial rate in these experiments follows a biphasic behavior, increasing due to the increment in substrate concentration ($MgATP^{2-}$) at different initial free Mg^{2+} concentrations and then falling due to the competitive inhibition by ATP^{4-} and/or to a decrease in free Mg^{2+} concentration (Figure 2). ATP^{4-} has been demonstrated to be a competitive inhibitor of Pfk-2 (*15*) and other kinases (*33*). It must be remarked that the

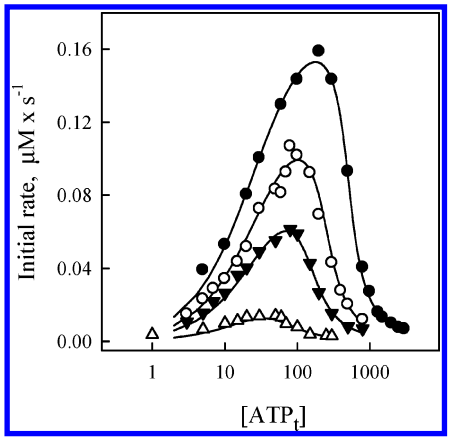

FIGURE 2: Initial velocities of the wild-type enzyme as a function of the ATP_t concentration at fixed Mg_t concentrations. The initial rates were obtained as a function of ATP_t with 500 μM (●), 250 μM (○), 150 μM (▼), and 50 μM (△) Mg_t. Symbols represent the experimental data while solid lines represent the simulated data obtained from the global fit to Model I ($r^2 = 0.9903$). The r^2 value and the simulated data obtained from the global fit to Model II were very similar to those obtained from Model I (data not shown). The enzymatic assay was performed with 0.0043 μM wild-type Pfk-2 (in terms of monomer subunit) at 26 °C in the presence of 1 mM of fructose-6-P. The ATP_t concentration is shown in logarithmic scale of micromolar concentration to better display the data fit.

concentration of $MgATP^{2-}$ never exceeded 0.5 mM, and hence allosteric inhibition can be ruled out. The initial rate profiles were adjusted collectively by global fit to rate equations in which different effects of ATP^{4-} and free Mg^{2+} were modeled (see Experimental Procedures). Two reaction mechanisms present good agreement with the data, as judged from r^2 values. Both of them consider a catalytic species which possesses another Mg^{2+} besides the divalent metal ion associated with ATP. While one of the mechanisms (Model I) involves competitive inhibition by ATP^{4-} and essential activation by Mg^{2+}, the other contemplates mixed activation by Mg^{2+} without competitive inhibition by ATP^{4-} (Model II). For the first model the kinetic parameters are $k_{cat} = 55\ s^{-1}$, $K_i(ATP^{4-}) = 2\ \mu M$, and $K_m(MgATP^{2-}) = 16\ \mu M$. These values are similar to those reported for Pfk-2 in our previous work. The binding constant of Mg^{2+} to the Pfk-2−fructose-6-P complex was 532 μM. In the second model, very similar values were obtained for k_{cat}, K_m(MgATP), and binding of Mg^{2+} to the Pfk-2−fructose-6-P complex. According to this model, Mg^{2+} could also bind to the Pfk-2−fructose-6-P−MgATP complex, with a constant of 102 μM. Other models, such as simple ATP^{4-} competitive inhibition (without activation by Mg^{2+}) or simple Mg^{2+} activation (without competitive inhibition by ATP^{4-}), failed to account for the experimental data (not shown). However, no matter the mechanism (Model I or II), a Mg^{2+} ion, other than the Mg^{2+} present in the nucleotide complex, is required for catalysis. Although we cannot discriminate between both models on the basis of the global fit of the data, we favor Model I since competitive inhibition by ATP^{4-} has been assessed kinetically (*15*). Then, we evaluate the involvement of the E190 residue from the NXXE motif of Pfk-2 in the binding of this activating Mg^{2+} ion at the active site. We choose the E residue because it appears to be the signature in that sequence pattern, since N could be replaced by S in AIR kinase from *Salmonella enterica* and 2-keto-3-deoxy-

Table 1: Kinetic Parameters of Wild-Type and E190Q Mutant Pfk-2 at Low and High Free Mg^{2+} Concentrations[a]

	wild type		E190Q	
	1 mM free Mg^{2+}	30 mM free Mg^{2+}	1 mM free Mg^{2+}	30 mM free Mg^{2+}
k_{cat}, s^{-1}	53 ± 2	53 ± 2	0.14 ± 0.04	1.43 ± 0.3
K_m(fructose-6-P), μM	100 ± 19	28 ± 2	10 ± 0.7	9.4 ± 0.5
K_m(MgATP), μM	20 ± 3	22 ± 5	149 ± 30	320 ± 12

[a] When assaying enzymatic activity versus fructose-6-P, $MgATP^{2-}$ was held constant at 1 and 2 mM for wild type and the E190Q mutant, respectively; when assaying versus $MgATP^{2-}$, fructose-6-P was held constant at 1 mM.

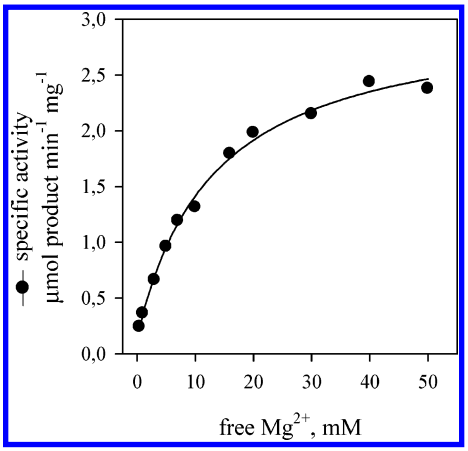

FIGURE 3: Effect of free Mg^{2+} concentration on the activity of the E190Q mutant Pfk-2. The activity of the E190Q mutant was measured as a function of the free Mg^{2+} concentration at 1 mM $MgATP^{2-}$ and 2 mM fructose-6-P. Specific activity is expressed as μmol of product min^{-1} mg^{-1}.

gluconate kinase from *Thermus thermophilus* (*34*, *35*) (Figure 1a). The E190Q mutant was expressed at high concentrations and was purified by employing the same protocol used with wild-type Pfk-2. Circular dichroism spectra from the mutant and wild-type enzymes were found to be virtually superimposable (data not shown), indicating that the mutation did not produce major changes in the secondary structure of the enzyme. Table 1 compares the kinetic properties of wild-type Pfk-2 and the E190Q mutant at 1 and 30 mM free Mg^{2+}. At 1 mM free Mg^{2+} the k_{cat} of the wild-type enzyme is about 400 times higher than E190Q k_{cat}. However, a 10-fold increment in the k_{cat} value of the E190Q mutant was observed when the free Mg^{2+} concentration was increased from 1 to 30 mM (Table 1). The reaction velocity of the E190Q mutant follows a hyperbolic dependence with the concentration of free Mg^{2+} at saturating concentrations of $MgATP^{2-}$ and fructose-6-P (Figure 3). A K_m value of 10 mM and a maximum velocity of 2.9 units/mg were obtained from a simple hyperbolic fit. Since E190Q activity declines with the decrease in free Mg^{2+} concentration and the trend points to zero activity when the concentration of free magnesium approaches zero, we inferred that the E190 residue participates in the positioning of the catalytic Mg ion at the active site. Table 1 shows a comparison of the effect of free Mg^{2+} concentration over the kinetic parameters of both enzymes. The mutant displayed a 15-fold decrease in K_m for $MgATP^{2-}$ at saturating concentrations of the divalent cation (Figure 4). The K_m for fructose-6-P is not affected by the binding of catalytic Mg^{2+} to the mutant enzyme; however, a decrement

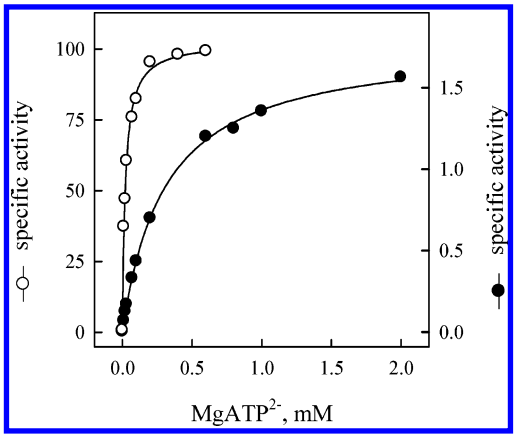

FIGURE 4: Initial velocity of wild-type and E190Q mutant Pfk-2 as a function of $MgATP^{2-}$ concentration. The reaction velocity of wild-type Pfk-2 (○) and the E190Q mutant (●) was measured as a function of $MgATP^{2-}$ at 30 mM free Mg^{2+} and 1 mM fructose-6-P. Specific activities are expressed as μmol of product min^{-1} mg^{-1}.

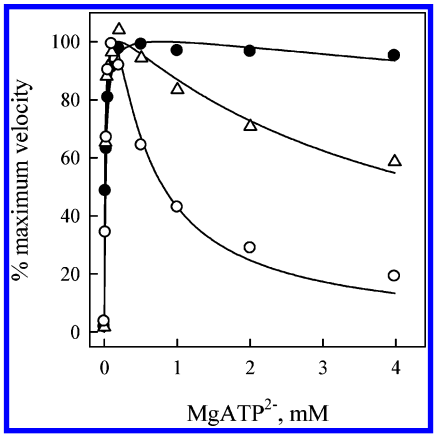

FIGURE 5: Effect of free Mg^{2+} and fructose-6-P on the $MgATP^{2-}$-induced inhibition of wild-type Pfk-2. Activity measurements were done at 0.1 mM fructose-6-P in the presence of 1 mM (○) and 30 mM (△) free Mg^{2+} and at 1 mM fructose-6-P in the presence of 1 mM free Mg^{2+} (●). Results are expressed as percent of enzymatic activity referred to the maximum value obtained for each condition.

is observed at high concentrations of the divalent cation in the wild type. This effect may possibly be correlated to the partial relief of the allosteric inhibition afforded by high concentrations of free Mg^{2+} (see below and Discussion).

Effect of Free Mg^{2+} on the Properties of the Allosteric Site of Pfk-2 and the E190Q Mutant. Allosteric binding of $MgATP^{2-}$ to dimeric Pfk-2 at low fructose-6-P concentrations (0.1 mM) results in inhibition of enzyme activity and tetramer formation, both of which can be reverted by increasing the sugar-P concentration (*15*, *16*, *36*). At free Mg^{2+} concentrations higher than that required to saturate the catalytic Mg^{2+} site, attenuation in $MgATP^{2-}$-induced inhibition is observed (Figure 5). This dual effect is analogous to the biphasic behavior reported for mammalian adenosine kinase: activation at the low concentration range of free Mg^{2+} and inhibition at concentrations over 1 mM. Under inhibitory conditions (0.1 mM fructose-6-P and 4 mM $MgATP^{2-}$), the enzymatic activity of Pfk-2 increases hyperbolically as a function of free Mg^{2+} concentration with a K_m close to 20 mM (data not shown). Also, we assessed whether this low-affinity effect of free Mg^{2+} affects the tetramerization induced by $MgATP^{2-}$ by performing size

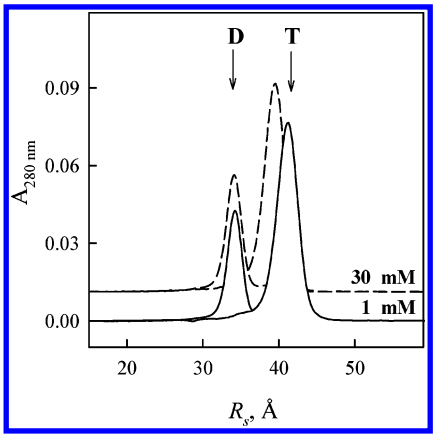

FIGURE 6: Effect of free Mg^{2+} concentration on the $MgATP^{2-}$-induced tetramerization of wild-type Pfk-2. The R_S of Pfk-2 was measured by size exclusion chromatography (see Experimental Procedures) in the absence (dimer) and in the presence (tetramer) of 0.1 mM $MgATP^{2-}$ at 1 mM (—) and 30 mM free Mg^{2+} (---). Protein elution was recorded as absorbance at 280 nm. T and D denote tetramer and dimer, respectively.

exclusion chromatography at low and high concentrations of the divalent cation. Figure 6 shows that in the absence of $MgATP^{2-}$, at 1 and 30 mM free Mg^{2+}, the Stokes radius of dimeric Pfk-2 is 31 Å, in agreement with previous measurements using dynamic light scattering (*37*). However, in the presence of 0.1 mM $MgATP^{2-}$, the species with the higher hydrodynamic volume decreases its Stokes radius when the experiment is performed at 30 mM free Mg^{2+} concentration. These results show that high concentrations of free Mg^{2+} affect both $MgATP^{2-}$-induced inhibition and tetramerization.

In the E190Q mutant, although allosteric inhibition occurs at concentrations of $MgATP^{2-}$ higher than that observed with the wild-type enzyme (Figure 7a), the increment in free Mg^{2+} from 1 to 30 mM partially attenuates this inhibition, resembling the wild-type behavior. Size exclusion chromatography in the presence of 0.2 mM $MgATP^{2-}$ (Figure 7b) demonstrates that binding $MgATP^{2-}$ to the allosteric site of the E190Q mutant is able to induce tetramerization, as seen in wild-type Pfk-2. However, a significant difference between the mutant and wild-type enzymes occurs at saturating concentrations of fructose-6-P (1 mM), where the inhibition by $MgATP^{2-}$ in the E190Q mutant is stronger than that observed for the wild-type enzyme.

Effect of Phosphate on the Kinetic Properties of Pfk-2 and the E190Q Mutant. Among the ribokinase family members, the activity of adenosine kinase from various sources, as well as bacterial ribokinase, is greatly affected by pentavalent ions (PVI) such as phosphate, arsenate, and vanadate (*20*, *38*, *39*). In the presence of these ions the maximum velocity increases and the K_m for the phosphate-accepting substrate decreases. It was also established that mutation of the N and E residues present in the NXXE motif from adenosine kinase resulted in proteins with a greatly altered response to phosphate.

We tested the effect of phosphate on the catalytic activity of Pfk-2 to determine whether it presents the same behavior observed in other ribokinase family members. Table 2 shows that 30 mM phosphate decreases the k_{cat} of wild-type Pfk-2 by 25%. However, sensitivity to phosphate inhibition is enhanced under subsaturating concentrations of fructose-6-P (0.2 mM) as shown in Figure 8a, where the increase in phosphate concentration up to 10 mM causes a 40% decrease

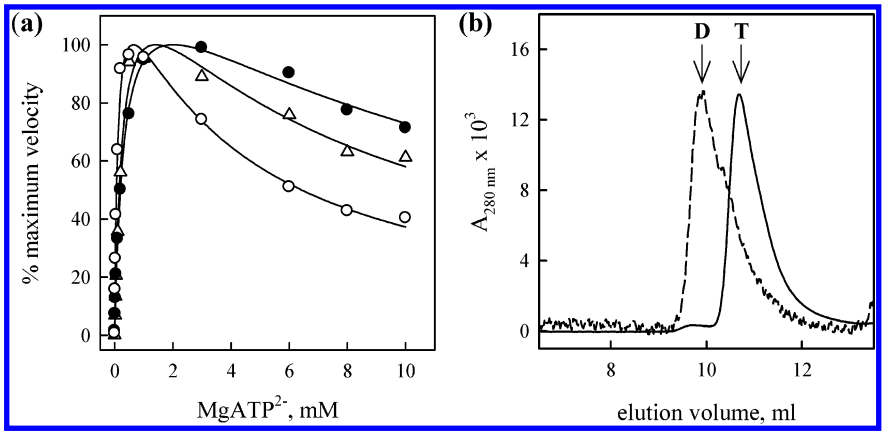

FIGURE 7: Effect of free Mg^{2+} and fructose-6-P concentrations on the $MgATP^{2-}$-induced inhibition of the E190Q mutant. (a) Activity measurements were performed at 0.1 mM fructose-6-P and 1 mM free Mg^{2+} (○), 0.1 mM fructose-6-P and 30 mM free Mg^{2+} (△), and 1 mM fructose-6-P and 1 mM free Mg^{2+} (●). (b) Elution profile from size exclusion chromatography of the E190Q mutant in the absence (---) and presence (—) of 0.2 mM $MgATP^{2-}$. T and D denote tetramer and dimer, respectively.

Table 2: Kinetic Parameters of Wild-Type and E190Q Mutant Pfk-2 in the Absence and Pesence of Phosphate at 5 mM Free Mg^{2+} [a]

	wild type		E190Q	
	control	30 mM PO_4^{3-}	control	30 mM PO_4^{3-}
k_{cat}, s^{-1}	53	40	0.46	0.18
	wild type		E190Q	
	control	10 mM PO_4^{3-}	control	10 mM PO_4^{3-}
K_m(fructose-6-P), μM	52	145[b]	18	88.5
K_m($MgATP^{2-}$), μM	15	16	190	210

[a] When assaying enzymatic activity versus fructose-6-P, $MgATP^{2-}$ was held constant at 1 and 2 mM for wild type and the E190Q mutant, respectively; when assaying versus $MgATP^{2-}$, fructose-6-P was held constant at 1 mM. [b] Corresponds to $K_{0.5}$ from a sigmoidal adjustment with $n_H = 1.9$.

of the enzymatic activity compared to the experiment performed at 1 mM fructose-6-P. We ruled out the possibility that phosphate was acting as a competitive inhibitor with respect to $MgATP^{2-}$ as a substrate, since this ion has no effect on the initial velocity when the assays were performed with this substrate at different phosphate concentrations (Figure 8a, inset; Table 2). Another possibility is that phosphate is acting as an inhibitor at low concentrations of both substrates due to binding at the allosteric site for $MgATP^{2-}$. To test this hypothesis, we observed the $MgATP^{2-}$-induced inhibition of wild-type Pfk-2 at 0.1 mM fructose-6-P in the presence of phosphate. Figure 8b shows that indeed PO_4^{3-} produces an extra inhibitory effect at all of the nucleotide concentrations studied, supporting the idea that phosphate is acting as an inhibitor at the allosteric site. Also, phosphate increases the K_m for fructose-6-P, while the K_m for $MgATP^{2-}$ remains unaffected in both wild-type and mutant enzymes. Surprisingly, at 10 mM phosphate the saturation curve for fructose-6-P changes from hyperbolic to a sigmoid response with a $K_{0.5}$ which is 3-fold higher than the corresponding one for the wild-type enzyme.

It is noteworthy that, at saturating fructose-6-P concentrations, the E190Q mutant displays a strong inhibition in the presence of 30 mM phosphate, since the activity is reduced to 40% of its original value (Table 2). Inhibition by phosphate is not dependent on free Mg^{2+} concentration (data not shown); hence an artifact due to the reduction of free Mg^{2+} required for enzyme activity by phosphate chelation can be legitimately ruled out. This result suggests that residue E190 is also contributing to the mechanism of phosphate inhibition in Pfk-2.

DISCUSSION

In this work we assess the influence of free Mg^{2+} and phosphate on Pfk-2 activity and allosteric regulation, considering them as general effectors of the members of the ribokinase family. On the basis of crystallographic data for adenosine kinase from *Toxoplasma gondii* and *Homo sapiens*, and ribokinase from *E. coli*, Maj et al. (*21*) made a composite model of the active site in which the positions of ligands and interactions with amino acid residues come from different structures. Particularly, one Mg^{2+} ion (from the human adenosine kinase structure) is interacting with N and E side chains of the NXXE motif, and a second one is assumed to bind the α- and β-phosphates from ATP substrate (as it does in *T. gondii* adenosine kinase). Whether these Mg^{2+} ions are involved in the observed activation and inhibition induced by free Mg^{2+} was not addressed. To evaluate the role of the E190 residue in Mg^{2+} and phosphate utilization by Pfk-2, we chose to replace it by Q because of its similar size and polarity but lack of negative charge on the side chain. In the case of Pfk-2 it is hard to model the interactions of ligands with the active site residues, due to the low percentage of identity with members of the ribokinase family with known structures. Considering that E from the NXXE motif is a strongly conserved active site residue, our kinetic results obtained with wild-type Pfk-2 and the E190Q mutant indicate that a Mg^{2+} ion present at the active site, additional to that present in the $MgATP^{2-}$ complex, is required for catalytic activity. Following the same reasoning of Maj et al. (*21*), the E190 residue should be part of the interactions that hold this catalytic Mg^{2+} at the active site. If phosphoryl transfer in Pfk-2 proceeds through the associative mechanism (S_N2-like), this divalent cation would be important for increasing the electrophilicity of the γ-phosphorus atom of the nucleotide by withdrawing charge via its interactions with the oxygen atoms, thus playing a role in forming the transition state of the reaction (*40*).

The E190Q mutant shows a hyperbolic increment of the enzymatic activity with the concentration of free Mg^{2+} with

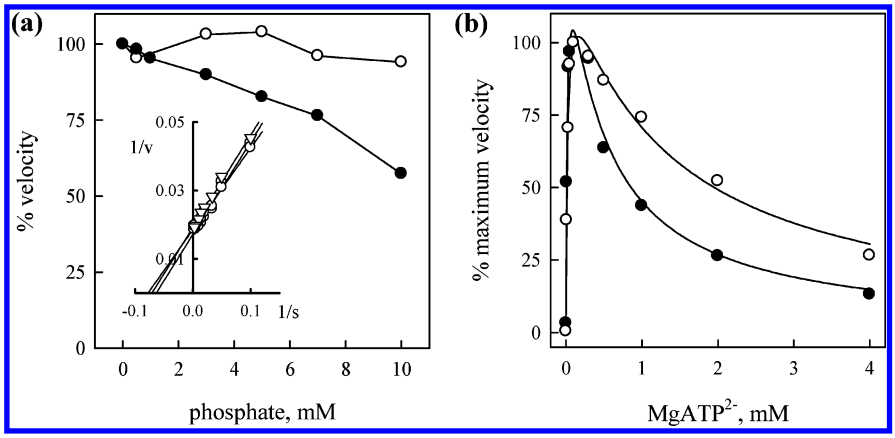

FIGURE 8: Effect of phosphate concentration on the initial velocity of wild-type Pfk-2. (a) Percentage of initial velocity as a function of phosphate concentration at saturating (1 mM) (○) and subsaturating (0.1 mM) (●) concentrations of fructose-6-P; $MgATP^{2-}$ was held constant at 0.2 mM. Inset: Double-reciprocal plot of initial velocity as a function of $MgATP^{2-}$ concentration at 0 (○), 5 (□), and 10 (△) mM phosphate, respectively. (b) $MgATP^{2-}$-induced inhibition in the absence (○) and in the presence (●) of 10 mM phosphate.

an activation constant of 10 mM (Figure 3). This value is considerably higher than any of the activation constants for Mg^{2+} obtained from global adjustment of the kinetic data of the wild-type enzyme. These results support the view that E190 from the NXXE motif of Pfk-2 is indeed involved in the binding of a catalytic Mg^{2+} at the active site. The requirement of a second metal ion for activity has been reported for phosphotransferases unrelated to the ribokinase family, such as phosphoenolpyruvate carboxykinase, pyruvate kinase, protein tyrosine kinase, and, recently, phosphofructokinase from *Ascaris suum* (*41*−*44*). In most of the cases the second Mg^{2+} stabilizes the transition state and facilitates catalysis; in the case of Pfk from *A. suum*, Mg^{2+} decreases the rate of release of MgATP from the E−MgATP−fructose-6-P complex, while in the kinase domain of the oncoprotein v-Fps the prominent role for free Mg^{2+} is to assist ATP−Mg binding by decreasing the dissociation constant. In *E. coli* Pfk-1 only one Mg^{2+} has been reported to bind at the active site, coordinated to the carboxylate group of an Asp residue (*26*). Regarding the ribokinase family and superfamily, our results support the view that the engagement of two Mg^{2+} ions at the active site is a general feature of the catalytic mechanism of all the members. In silico calculations of the phosphoryl transfer reaction in Thz kinase, a distant relative that belongs to the superfamily, lead to the conclusion that two magnesium ions seem to be important for preferential transition state stabilization and lowering of the activation barrier (*45*).

In contrast to the inhibition observed among other members of the ribokinase family, high concentrations of Mg^{2+} alleviate the allosteric inhibition induced by $MgATP^{2-}$. The reduction observed in the Stokes radius of the high molecular weight species at 30 mM free Mg^{2+} may result from either fast dimer−tetramer equilibrium or compaction of the tetrameric form. These low-affinity effects of free Mg^{2+} could be due to a competition for the allosteric site between this ion and $MgATP^{2-}$. Since a reduction in the apparent K_m for fructose-6-P in the wild-type enzyme is seen at 30 mM free Mg^{2+}, we suggest that this might be an indirect consequence of the displacement of $MgATP^{2-}$ from the allosteric site, which is expected to bind at $MgATP^{2-}$ concentrations over 0.5 mM. In the E190Q mutant, higher concentrations of $MgATP^{2-}$ are required to achieve inhibition. However, although inhibition is alleviated to some extent by increments in free Mg^{2+} and fructose-6-P concentrations, the mutant enzyme displays a strong inhibition even at saturating concentrations of fructose-6-P, as opposed to the behavior observed with the wild-type enzyme.

Phosphate increases the activity of phosphofructokinases from yeast, *A. suum*, erythrocytes, and muscle and nervous tissues of vertebrates and invertebrates, as well as the activity of liver 6-phosphofructo-2-kinase (*46*−*50*). Regarding the ribokinase family, this ion is an activator of ribokinase (*20*) and adenosine kinase (*21*). Park et al. (*51*) suggested that the mechanism of activation by phosphate in adenosine kinase involves a direct participation in the reaction, facilitating the transfer of γ-phosphate from ATP to adenosine. This led to the suggestion that PVI dependency could be a general feature of sugar kinases, including members of the ribokinase family and other families (*21*).

Wild-type Pfk-2 displays inhibition by phosphate at high concentrations, and the replacement of Glu190 by Gln in the NXXE motif increases this effect (Table 2). It is noteworthy that under subsaturating fructose-6-P concentrations phosphate inhibition is enhanced, resembling the allosteric effect of $MgATP^{2-}$. Since we ruled out the possibility that phosphate might be acting as a competitive inhibitor of $MgATP^{2-}$ at the active site, we hypothesized that phosphate is acting at the level of the allosteric site. In agreement with this, we observed an extra inhibitory effect over the $MgATP^{2-}$-induced inhibition in the presence of phosphate. Although phosphate ion has been described as an activator for most of the phosphofructokinases studied, for the enzyme from a hibernating ground squirrel a decrease in temperature alone causes a change of inorganic phosphate from activator to inhibitor (*52*). The K_m for fructose-6-P is increased by phosphate in both wild-type and Pfk-2 mutant enzymes. If phosphate and $MgATP^{2-}$ were binding to the same site in *E. coli* Pfk-2, it is tempting to suggest the evolutionary origin of the allosteric site as derived from the phosphate site characterized in several members of the ribokinase family.

The results presented in this work indicate that E190 from the NXXE motif of *E. coli* Pfk-2 is required for proper binding of a Mg^{2+} ion at the active site and points to the existence of a catalytic Mg^{2+} at the active site, other than the Mg^{2+} ion present in the metal−nucleotide complex. Kinetic data obtained with the E190Q mutant indicate that

proper Mg^{2+} binding is required for catalysis. The low-affinity effect of free Mg^{2+} over the allosteric inhibition and tetramer properties suggests a competition with $MgATP^{2-}$ at the allosteric site. While typically considered an activator of phosphofructokinase and ribokinase family members, inorganic phosphate performed as an inhibitor of Pfk-2, probably acting at the allosteric site. Work is in progress in order to establish the specific roles of the NXXE motif residues in the allosteric inhibition of Pfk-2.

REFERENCES

1. Bork, P., Sander, C., and Valencia, A. (1993) Convergent evolution of similar enzymatic function on different protein folds: the hexokinase, ribokinase, and galactokinase families of sugar kinases, *Protein Sci. 2*, 31−40.
2. Wu, L.-F., Reizer, A., Reizer, J., Cai, B., Tomich, J. M., and Saier, M. H. (1991) Nucleotide sequence of the *Rhodobacter capsulatus fruK* gene, which encodes fructose-1-phosphate: evidence for a kinase superfamily including both phosphofructokinases of *Escherichia coli*, *J. Bacteriol. 173*, 3117−3127.
3. Sigrell, J. A., Cameron, A. D., Jones, A. J.. and Mowbray, S. L. (1998) Structure of *Escherichia coli* ribokinase in complex with ribose and dinucleotide determined to 1.8 Å resolution: insights into a new family of kinase structure, *Structure 6*, 183−193.
4. Sigrell, J. A., Cameron, A. D., and Mowbray, S. L. (1999) Induced fit on sugar binding activates ribokinase, *J. Mol. Biol. 290*, 1009−1018.
5. Mathews, I. I., Erion, M. D., and Ealick, S. E. (1998) Structure of human adenosine kinase at 1.5 Å resolution, *Biochemistry 37*, 15607−15620.
6. Schumacher, M. A., Scott, D. M., Mathews, I. I., Ealick, S. E., Roos, D. S., Ullman, B., and Brennan, R. G. (2000) Crystal structures of *Toxoplasma gondii* adenosine kinase reveal a novel catalytic mechanism and prodrug binding, *J. Mol. Biol. 296*, 549−567.
7. Tsuge, T., Sakuraba, H., Kobe, T., Kujime, A., Katunuma, N., and Ohshima, T. (2002) Crystal structure of the ADP-dependent glucokinase from *Pyrococcus horikoshii* at 2.0-Å resolution: A large conformational change in ADP-dependent glucokinase, *Protein Sci. 11*, 2456−2463.
8. Zhang, Y., Dougherty, M., Downs, D. M., and Ealick, S. E. (2004) Crystal structure of an aminoimidazole riboside kinase from *Salmonella enterica*: implications for the evolution of the ribokinase superfamily, *Structure 12*, 1809−1821.
9. Safo, M. K., Musayev, F. N., Hunt, S., di Salvo, M. L., Scarsdale, N., and Schirch, V. (2004) Crystal structure of the PdxY protein from *Escherichia coli*, *J. Bacteriol. 186*, 8074−8082.
10. Campobasso, N., Mathews, I., Begley, T. P., and Ealick, S. E. (2000) Crystal structure of 4-methyl-5-β-hydroyethylthiazole kinase from *Bacillus subtilis* at 1.5 Å resolution, *Biochemistry 39*, 7868−7877.
11. Cheng, G., Bennett, E. M., Begley, T. P., and Ealick, S. E. (2002) Crystal structure of 4-amino-5-hydroxymethyl-2-methylpyrimidine phosphate kinase from *Salmonella typhimurium* at 2.3 Å resolution, *Structure 10*, 225−235.
12. Ito, S., Fushinobu, S., Yoshioka, I., Koga, S., Matsuzawa, H., and Wakagi, T. (2001) Structural basis for the ADP-specificity of a novel glucokinase from hyperthermophilic archaeon, *Structure 9*, 205−214.
13. Ito, S., Fushinobu, S., Jeong, J.-J., Yoshioka, I., Koga, S., Shoun, H., and Wakagi, T. (2003) Crystal structure of an ADP-dependent glucokinase from *Pyrococcus furiosus*: implications for a sugar-induced conformational change in ADP-dependent kinase, *J. Mol. Biol. 331*, 871−883.
14. Tuininga, J. E., Verhees, C. H., van der Oost, J., Kengen, S. W. M., Stams, A. J. M., and de Vos, W. M. (1999) Molecular and biochemical characterization of the ADP-dependent phosphofructokinase from the hyperthermophilic archaeon *Pyrococcus furiosus*, *J. Biol. Chem. 274*, 21023−21028.
15. Guixé, V., and Babul, J. (1985) Effect of ATP on phosphofructokinase-2 from *Escherichia coli*. A mutant enzyme altered in the allosteric site for MgATP, *J. Biol. Chem. 260*, 11001−11005.
16. Guixé, V., and Babul, J. (1988) Influence of ligands on the aggregation of the normal and mutant forms of phosphofructokinase-2 of *Escherichia coli*, *Arch. Biochem. Biophys. 264*, 519−524.
17. Guixé, V., Rodríguez, P. H., and Babul, J. (1998) Ligand-induced conformational transitions in *Escherichia coli* phosphofructokinase-2: evidence for an allosteric site for MgATP, *Biochemistry 37*, 13269−13275.
18. Cabrera, R., Fischer, H., Trapani, S., Craievich, A. F., Garratt, R. C., Guixé, V., and Babul, J. (2003) Domain motions and quaternary packing of phosphofructokinase-2 from *Escherichia coli* studied by small angle X-ray scattering and homology modeling, *J. Biol. Chem. 278*, 12913−12919.
19. Andersson, C. E., and Mowbray, S. L. (2002) Activation of ribokinase by monovalent cations, *J. Mol. Biol. 315*, 409−419.
20. Maj, M. C., and Gupta, R. S. (2001) The effect of inorganic phosphate on the activity of bacterial ribokinase, *J. Protein Chem. 20*, 139−144.
21. Maj, M. C., Singh, B., and Gupta, R. S. (2002) Pentavalent ions dependency is a conserved property of adenosine kinase from diverse sources: identification of a novel motif implicated in phosphate and magnesium ion binding and substrate inhibition, *Biochemistry 41*, 4059−4069.
22. Fisher, M. N., and Newsholme, E. A. (1984) Properties of rat heart adenosine kinase, *Biochem. J. 221*, 521−528.
23. Baek, Y. H., and Nowak, T. (1982) Kinetic evidence for a dual cation role for muscle pyruvate kinase, *Arch. Biochem. Biophys. 217*, 491−497.
24. Lee, M. H., Hebda, C. A., and Nowak, T. (1981) The role of cations in avian liver phosphoenolpyruvate carboxykinase catalysis. Activation and regulation, *J. Biol. Chem. 256*, 12793−12801.
25. Waas, W., and Dalby, K. N. (2003) Physiological concentrations of divalent magnesium ion activate the serine/threonine specific protein kinase ERK2, *Biochemistry 42*, 2960−2970.
26. Berger, S. A., and Evans, P. R. (1992) Site-directed mutagenesis identifies catalytic residues in the active site of *Escherichia coli* phosphofructokinase, *Biochemistry 31*, 9237−9242.
27. Daldal, F. (1983) Molecular cloning of the gene for phosphofructokinase-2 of *Escherichia coli* and the nature of a mutation pfkB1, causing high level of the enzyme, *J. Mol. Biol. 168*, 285−305.
28. Tabor, S., and Richardson, C. C. (1985) A bacteriophage T7 RNA polymerase/promoter system for controlled exclusive expression of specific genes, *Proc. Natl. Acad. Sci. U.S.A. 82*, 1074−1078.
29. Babul, J. (1978) Phosphofructokinases from *Escherichia coli*. Purification and characterization of the nonallosteric isozyme, *J. Biol. Chem. 253*, 4350−4355.
30. Gaffney, T. J., and O'Sullivan, W. J. (1964) Kinetic studies of the activation of adenosine triphosphate-lombricine transferase by magnesium ions, *Biochem. J. 90*, 177−181.
31. Segel, I. H. (1975) *Enzyme kinetics. Behavior and analysis of rapid equilibrium and steady-state enzyme systems*, John Wiley & Sons, New York.
32. Cornish-Bowden, A. (1995) *Fundamentals of enzyme kinetics*, Portland Press Ltd., London.
33. Morrison, J. F. (1979) Approaches to kinetic studies on metal-activated enzymes, *Methods Enzymol. 63*, 257−294.
34. Zhang, Y., Dougherty, M., Downs, D. M., and Ealick, S. E. (2004) Crystal structure of an aminoimidazole riboside kinase from *Salmonella enterica*: implications for the evolution of the ribokinase superfamily, *Strutcure 12*, 1809−1821.
35. Ohshima, N., Inagaki, E., Yasuike, K., Takio, K., and Tahirov, T. H. (2004) Structure of *Thermus thermophilus* 2-keto-3-deoxygluconate kinase: evidence for recognition of an open chain substrate, *J. Mol. Biol. 340*, 477−489.
36. Kotlarz, D., and Buc, H. (1981) Regulatory properties of phosphofructokinase-2 from *Escherichia coli*, *Eur. J. Biochem. 117*, 569−574.
37. Cabrera, R., Guixé, V., Alfaro, J., Rodríguez, P. H., and Babul, J. (2002) Ligand-dependent structural changes and limited proteolysis of *Escherichia coli* phosphofructokinase-2, *Arch. Biochem. Biophys. 406*, 289−295.
38. Maj, M. C., Singh, B., and Gupta, R. S. (2000) Structure−activity studies on mammalian adenosine kinase, *Biochem. Biophys. Res. Commun. 275*, 386−393.
39. Hao, W., and Gupta, R. S. (1996) Pentavalent ions dependency of mammalian adenosine kinase, *Biochem. Mol. Biol. Int. 38*, 889−899.

40. Matte, A., Tari, L. W., and Delbaere, L. (1998) How do kinases transfer phosphoryl groups?, *Structure 6*, 413−419.
41. Colombo, G., Carlson, G. M., and Lardy, H. A. (1981) Phosphoenolpyruvate carboxykinase (guanosine 5′-triphosphate) from rat liver cytosol. Dual-cation requirement for the carboxylation reaction, *Biochemistry 20*, 2749−2757.
42. Sun, G. S., and Budde, R. J. A. (1997) Requirement for an additional divalent metal cation to activate protein tyrosine kinases, *Biochemistry 36*, 2139−2146.
43. Boehr, D. D., Thompson, P. R., and Wright, G. D. (2001) Molecular mechanism of aminoglycoside antibiotic kinase APH(3′)-IIIa. Roles of conserved active site residues, *J. Biol. Chem. 276*, 23929−23936.
44. Gibson. G. E., Harris, B. G., and Cook, P. F. (2006) Optimum activity of the phosphofructokinase from *Ascaris suum* requires more than one metal ion, *Biochemistry 45*, 2453−2460.
45. Dyguda, E., Szefczyk, W., and Sokalski (2004) The mechanism of phosphoryl transfer reaction and the role of active site residues on the basis of ribokinase-like kinases, *Int. J. Mol. Sci. 5*, 141−153.
46. Bañuelos, M., Gancedo, C., and Gancedo, J. (1977) Activation by phosphate of yeast phosphofructokinase, *J. Biol. Chem. 252*, 6394−6398.
47. Hofer, H. W., Allen, B. L., Kaeini, M. R., Pette, D. P., and Harris, B. G. (1982) Phosphofructokinase from *Ascaris suum*. Regulatory kinetic studies and activity near physiological conditions, *J. Biol. Chem. 257*, 3801−3806.
48. Kuhn, B., Jacobash, G., and Rapoport, S. M. (1974) Identity of sulfate and phosphate activation of the phosphofructokinase from erythrocytes, *FEBS Lett. 38*, 354−356.
49. Sugden, P. H., and Newsholme, E. A. (1975) The effects of ammonium, inorganic phosphate and potassium ions on the activity of phosphofructokinases from muscle and nervous tissues of vertebrates and invertebrates, *Biochem. J. 150*, 113−122.
50. Laloux, M., Van Schaftingen, E., Francois, J., and Hers, H. G. (1985) Phosphate dependency of phosphofructokinase 2, *Eur. J. Biochem. 148*, 155−159.
51. Park, J., Singh, B., Maj, M. C., and Gupta, R. S. (2004) Phosphorylated derivatives that activate or inhibit mammalian adenosine kinase provide insights into the role of pentavalent ions in AK catalysis, *Protein J. 23*, 167−177.
52. MacDonald, J. A., and Storey, K. B. (2005) Temperature and phosphate effects on allosteric phenomena of phosphofructokinase from a hibernating ground squirrel (*Spermophilus lateralis*), *FEBS J. 272*, 120−128.

BI060026O